**ATLAS Internal Note**
**INDET-NO-166**
**17 April 1997**

# Status report on modules cooling and mechanics

G. Barbier*, P. Bonneau**, Ph. Bouvier*, M. Bosteels**, A. G. Clark*, Ph. Demierre*, A. R. Holmes***. G. Tappern****, Perrin*, B. Vuaridel*, M. Weber*

*DPNC, University of Geneva, 24, quai E. Ansermet 1211 Genève 4.
**CERN, 1211 Genève 23.
*** Dept. of Physics, University of Oxford, UK
**** Rutherford Laboratory, UK

**Abstract:** The design and the prototyping of the Atlas Silicon Tracker (SCT) barrel is reported in this technical note. A prototype mechanical design is presented, together with the demonstration of a technique to precisely mount and subsequently cool the electronics modules.

## 1 Introduction

Presented here is the design and prototyping of an ultra-light mechanical structure to support silicon microstrip detectors for the SCT barrel, with readout electronics cooling with the high mechanical precision needed for the LHC Atlas tracker. Owing to high radiation doses in the LHC environment, the detectors have to be maintained at low temperature, typically below zero degree Celsius in order to survive (ATL94). The prototyping started in 1995, whilst baselines were not defined. The options followed here do not always follow today's standard baselines of Atlas. However, most of the results can be adapted to other designs, including Atlas baseline choices.

A mechanical structure has been chosen, made of carbon fiber sandwich cylinders. Such structures can be manufactured to have a very small coefficient of thermal expansion (CTE). This mechanical property is fundamental since the SCT will operate at a temperature below 0°C. It will allow for an accurate module assembly at room temperature whilst the negligible thermal expansion will preserve the module positions at the lower operating temperatures. Furthermore, a small temperature gradient of a few degrees can exist across the structure without affecting the alignment.

At first only individual module assembly was considered. This includes some desirable features, i.e., the possibility to pre-install and test the cables, the cooling system and the precisely aligned supports for an easier installation and replacement of the modules. In this scheme, inserts are glued onto the carbon sandwich barrel and then machined down to the required accuracy. This is probably the most inexpensive but elegant way to reach the desired mechanical accuracy. Later "local supports" were also introduced in design studies.

The cooling of the detectors and of the associated electronics is provided by a coolant in an aluminum tube. Since the CTE of aluminum does not match the one of the barrel structure, the tube is allowed to slide in order to avoid mechanical stress to be transmitted on the structure. This is possible, in the scheme presented here, with a silicone compound joint between the cooling pipe and the modules.

For historical reasons, most prototypes have something in common with the Z-modules type. However, design studies were performed to show that the mechanical solution presented here can be applied to any kind of modules as well as to local supports. In addition, a very attractive "center tap" module with TPG has been separately investigated in detail.

## 2 Mechanical Structure

Four carbon fiber composite sandwich cylinders were chosen as the support structure for the four layers of silicon detectors forming the SCT barrel. This type of structure exhibits a very high specific stiffness (or very high $E \bullet X_0$ product) coupled with a high dimensional stability and a very near zero coefficient of thermal expansion (CTE), smaller than 0.5 ppm/°C. Module precise fixation points, cooling pipes and cables can be pre-installed and tested prior module installation. Alternatively, the concept of local support (sub assembly of 6 or 12 modules) can be relatively simply introduced in the design as an intermediate step between modules and cylinder. The aim of the local support is to be able to have a more modular assembly scenario where six or twelve modules can be fully tested including thermal cycling prior to assembly on the barrel with a cost impact on the material budget. The advantages of individual module assembly versus local support is an highly debated topic in the collaboration and is out of the scope of this technical report.

## 2.1 Sandwich cylinder

A sandwich type of construction was chosen for its high specific bending stiffness. This also offers sufficient local stiffness to allow for the machining of precision inserts which are integrated in the sandwich to provide fixation points for the detectors module or local supports. Moreover, in such a structure, the material is very evenly distributed.

The choice of the type of carbon-fiber/cyanate ester system was driven by the required stiffness and the possibility to obtain an in plane CTE of 0 +/- 0.5 ppm/°C. A cyanate ester resin, of the type used for stable structure applications in space, was chosen to minimize potential distortions induced by moisture intake and release. This kind of product also offers the advantage of being available in very thin prepreg forms, permitting the quasi-isotropic 0/60/-60/-60/60/0 lay-up of the skins.

The design aims for a sandwich of less than 1.2kg/m2 aerial weight with quasi isotropic laid up skins giving 0.265%Xo per cylinder at 90 degrees.

End flanges were introduced in the design at both ends of the cylinders, as shown in fig. 1, This adds considerable circumferential stiffness and provides location for the fixations of the structures interlinking the four cylinders together. Extra handling points can also be implemented in these flanges.
Several simulations were made to optimize the cylinder design. The deflection of each of the four barrels is less than 10 microns under the load represented by the detectors with the additional stiffness provided by end flanges, see fig. 2. In the simulation, the barrels were supported by four points in the mid plane (2 each end).

A cheap and widely used Nomex ® honeycomb core was considered first and tested giving reasonably good results. The small distortions induced by CTE mismatch with skins are shown in fig. 3. An alternative carbon fiber/cyanate ester honeycomb is also considered. This solution was tested on flat panels, as shown in figs 12, 13. However its price is far higher and the processing requires that the core is heat formed to a cylindrical shape.

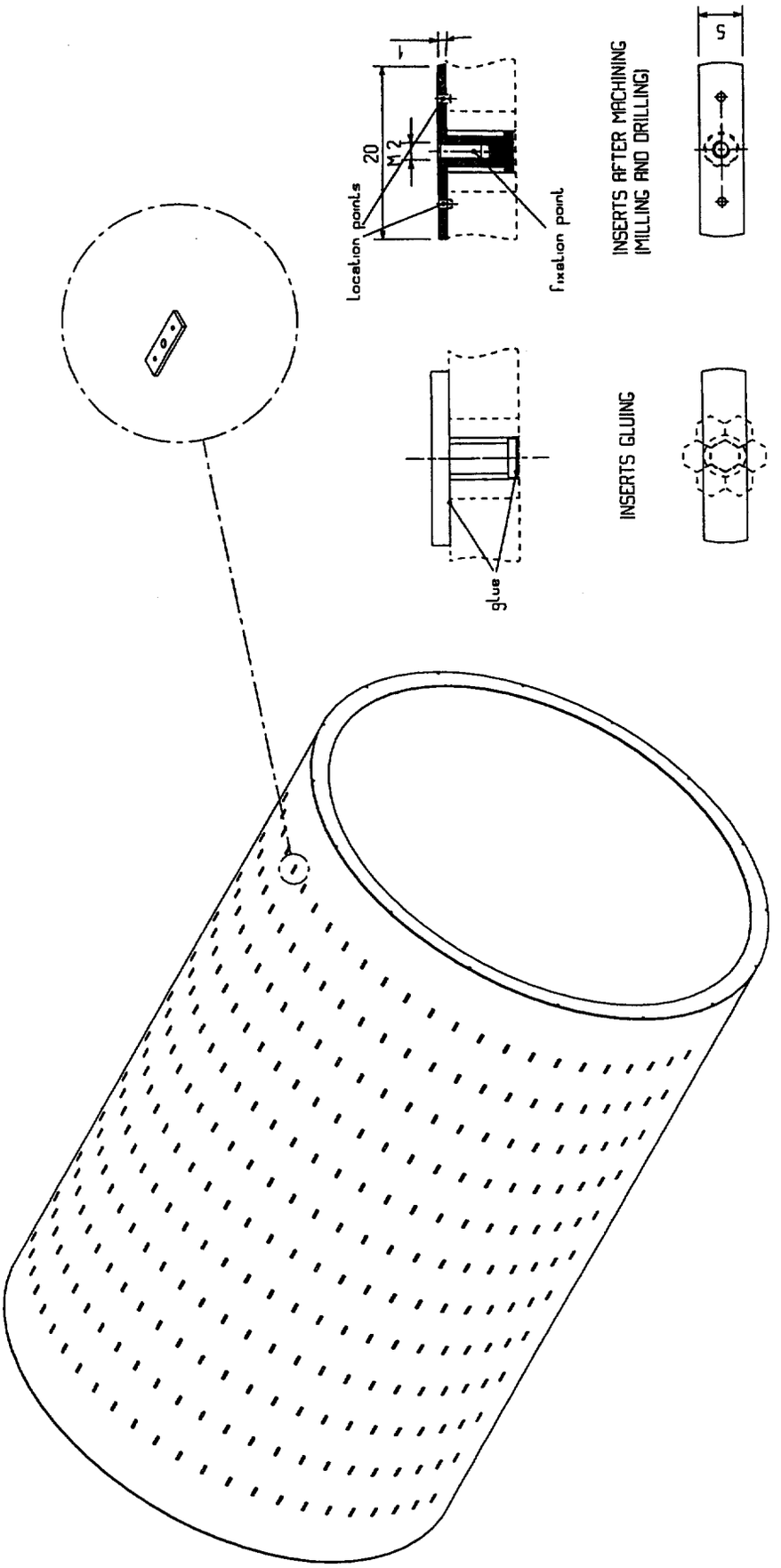


fig. 1 CFRP cylinder with end flanges and inserts to fasten silicon modules and cooling pipes.

Attempts were made on small samples to minimize the amount of adhesive between prepolimerized skins and the core of the sandwich. Results showed that with less than 100g/m2 of glue, skin core adhesion was marginal. Great care in sandwich design should be taken to avoid peeling of the skins which can easily occur with thin high modulus fiber skins.

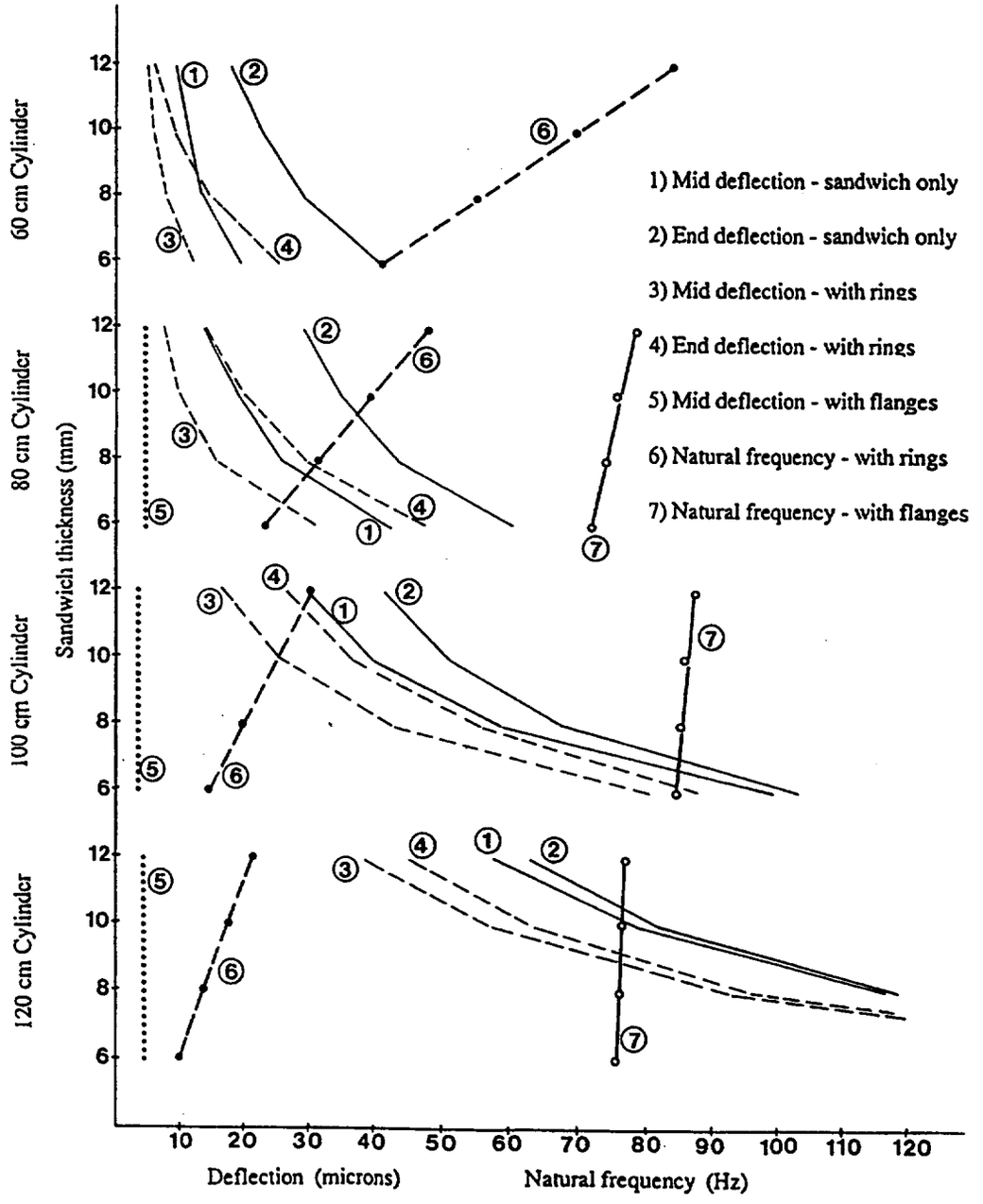


fig. 2 Diagram showing deflections and natural frequencies of the four CFRP cylinders of the Atlas SCT with diameter 60, 80, 100 and 120 cm. With flanges, the deflection is less than 10 μm under its own weight and the module load, as shown by curves 5, while the natural frequency is above 70 Hz, as shown by curves 7.

Co-curing was also tested on some heavier samples with 8 ply lay-up skins (0/45/-45/90/90/-45/45/0). For the cylinder, the exact choice of manufacturing process will be discussed and agreed with the manufacturer.

Dimension stability tests were performed on a Nomex-core sandwich sample submitted to an environmental change from typical assembly lab condition (20°C ~50% RH) to 20°C in dry

nitrogen atmosphere. Results showing no measurable effect, at the limiting measurement precision of about 5 μm, are shown in fig 4.

Lightweight inserts, see fig.1, for fastening the modules were specially developed and prototyped in aluminum. Great care was taken to glue them on both skins of the test sandwich panel avoiding use of potting compounds for material budget reasons. For production, an alternative lighter insert material is foreseen, for example, short fiber reinforced moldings.

### 2.2 Module attachment

Several design and prototypes studies were made of attaching silicon modules to the dimensionally stable cfrp cylinder with suitable cooling. Since attachment and cooling are vital, studies were made for the different types of modules considered by Atlas, to demonstrate the compatibility of the present design.
Two alternative mounting techniques were considered, one where modules are mounted individually, directly on the cylinder as shown in fig. 5, and another implementing a local support subassembly of 6 or 12 modules, which is then attached to the cylinder as shown in fig. 6 with the 6-modules local supports.

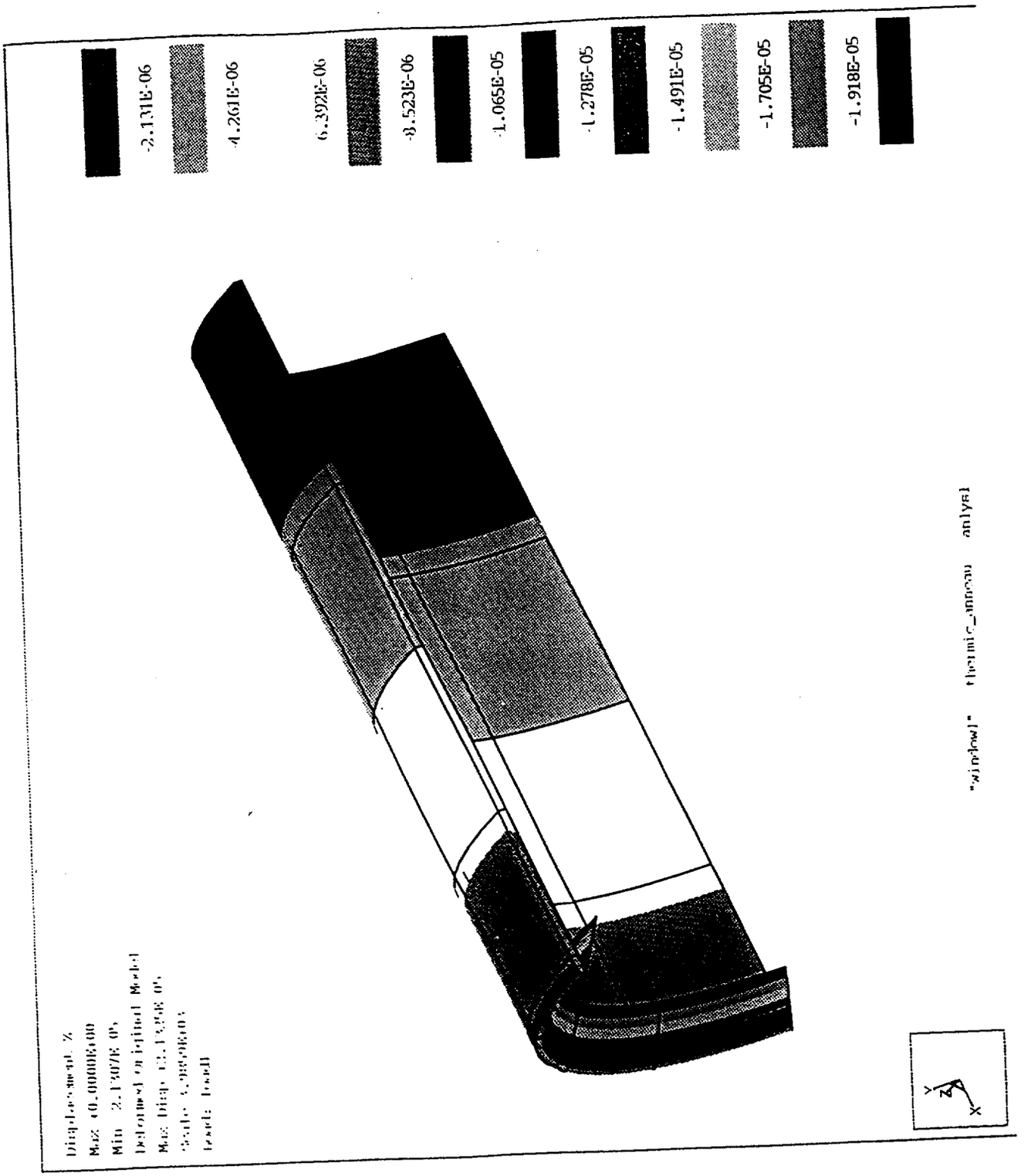


Fig. 3 Structure of the cylinder with end flanges. The different gray tones represents relative displacements after the structure has been cooled.

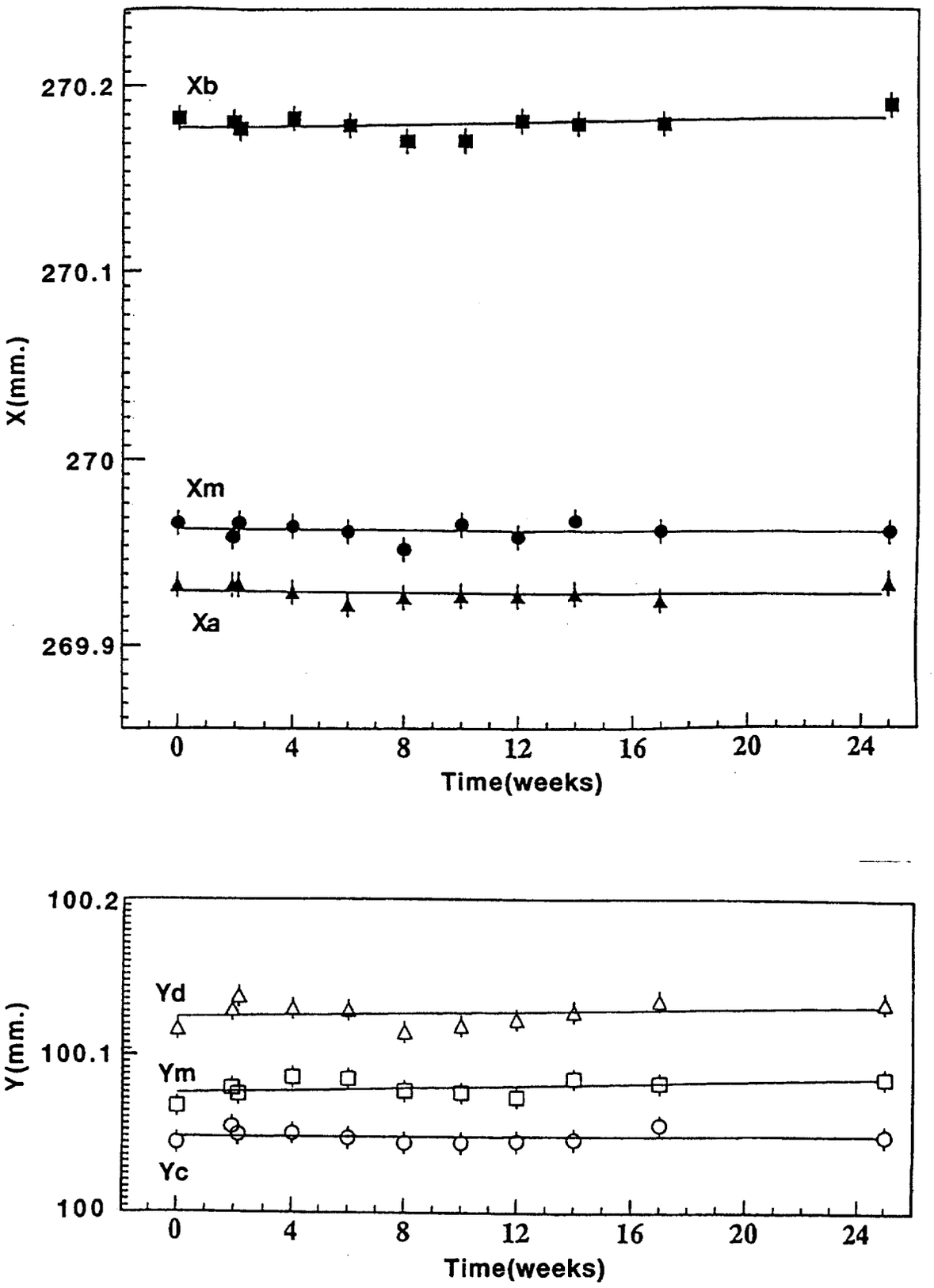


fig. 4 Long term mechanical stability in dry nitrogen of the X-Y dimensions between reference marks of a Nomex cored sandwich sample (RS3/XN50), skin in 0/45/-45/90/90/-45/45/0 lay-up.

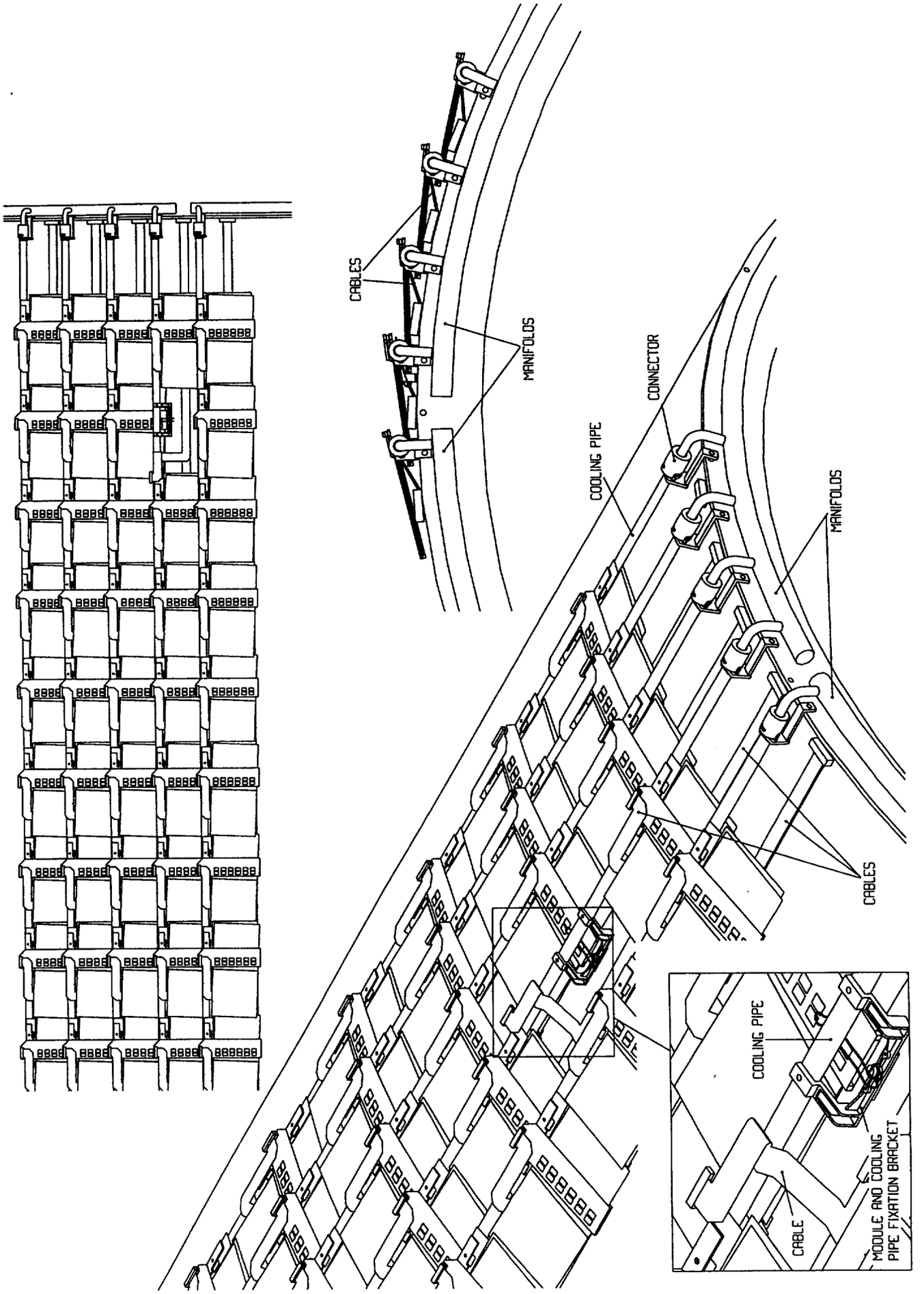


fig. 5 Modules mounted individually directly on the sandwich cylinder.

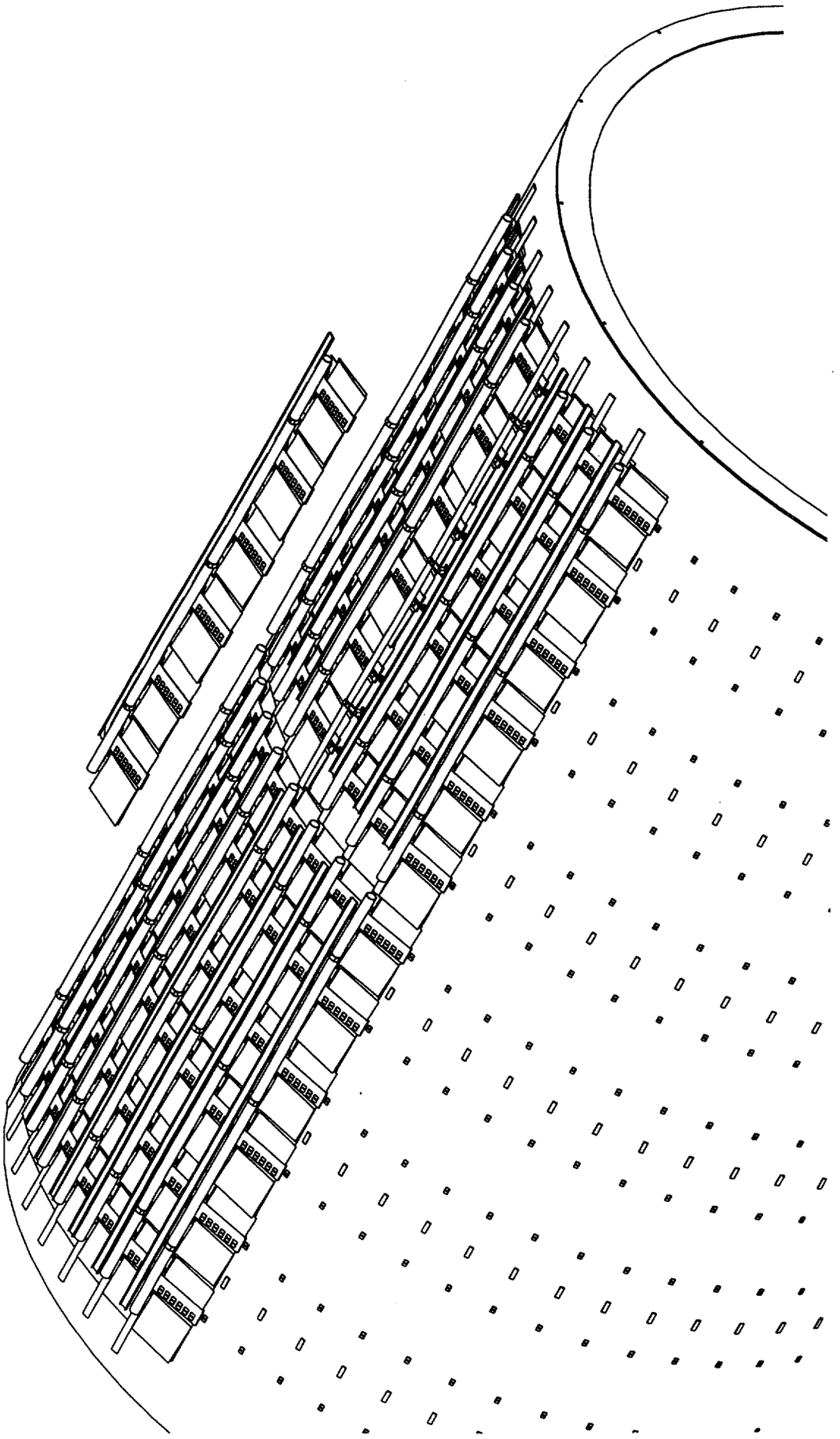

fig. 6 Local support subassembly of 6 or 12 modules, which is then attached to the cylinder.

## 3 Module cooling

The cooling system chosen here is a leakless® Cooling System (LCS) in which the fluid is below atmospheric pressure to keep the risk of flooding small. It consists of parallel aluminum tubes, one per module row, running along the z-direction of the barrel, as shown in fig.7, and filled with a fluid, e.g. a mixture of water and Glycol or water and Methanol. The system was designed to have a pressure drop of ≈ 200 mbar along the 1.6m long tube, @ 25 l/h (Bon94, Bon95). For the test, a 2kW cooling unit was operating at temperatures between approximately -20 °C and -10 °C. Note that, the fluid could be replaced by « binary ice » to keep a more homogeneous temperature along the tubes. Since the flow and pressure drop considered for the « binary ice » solution are about the same as the one presented here, the tubes specifications are similar for both types of cooling. A manifold system where all the pipes are grouped by a quarter of a barrel is shown in fig.7. This represents the simplest way to have a truly leakless® system were it is possible to remove all the fluid when the tube is dismounted. Detailed studies were made, allowing for the aluminum tube to expand and shrink freely without transmitting stress to either modules or cfrp cylinder. Thermal contact is made more effective by the use of silicon heat sink compound or "thermal grease".

### 3.1 Tube design

#### 3.1.1 Round tube

The first tube we investigated was round, 3mm O.D and 2.6mm I.D. An initial cooling measurement on a round tube at room temperature was performed, with a 1m long round tube, with a constant heat load of 40W (about the same heat load per length for 60W and the barrel length of 1,6). The average temperature of the water was measured at the entrance, $T_{in}$, and at the exit of the tube, $T_{out}$. In addition the wall temperatures were measured at both ends of the tube, $T_{Win}$, $T_{Wout}$. An almost constant temperature gradient, $\Delta T = T_{Wout} - T_{out}$, is observed between the wall temperature and the average fluid temperature. This temperature gradient is independent of the flux over a large range were the flux is probably laminar, as shown by the data of fig.8 For an average fluid temperature at the exit of the tube, $T_{out}$, the aluminum tube is about 3.5°C warmer. Since it does not depend on the flow, this is interpreted in terms of a gradient across the fluid, due to the poor thermal conductivity of water. At the higher flux the flow becomes turbulent and the gradient becomes much smaller. One could consider turbulent flow to reduce the temperature gradient, however this could only be done with a higher pressure drop to flow ratio and that is incompatible with the 200 mbar design rule for a leakless® system.

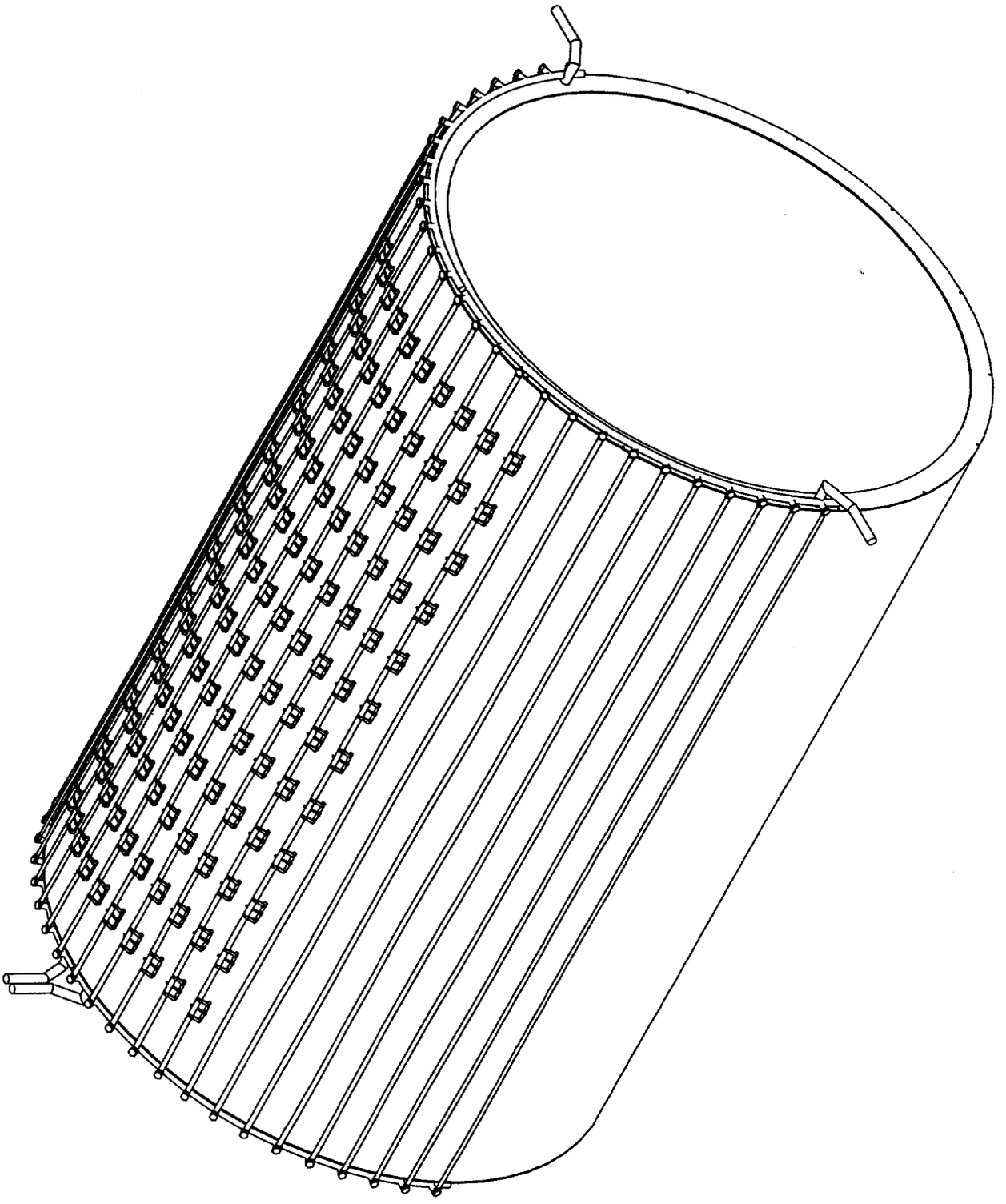

fig. 7 Schematic representation of a fraction of the barrel showing the cooling of the modules with one tube per module row. Manifolding of the cooling tube by quarter. This is the simplest way to reduce air pockets in the system and to allow an easy filling and draining of the system.

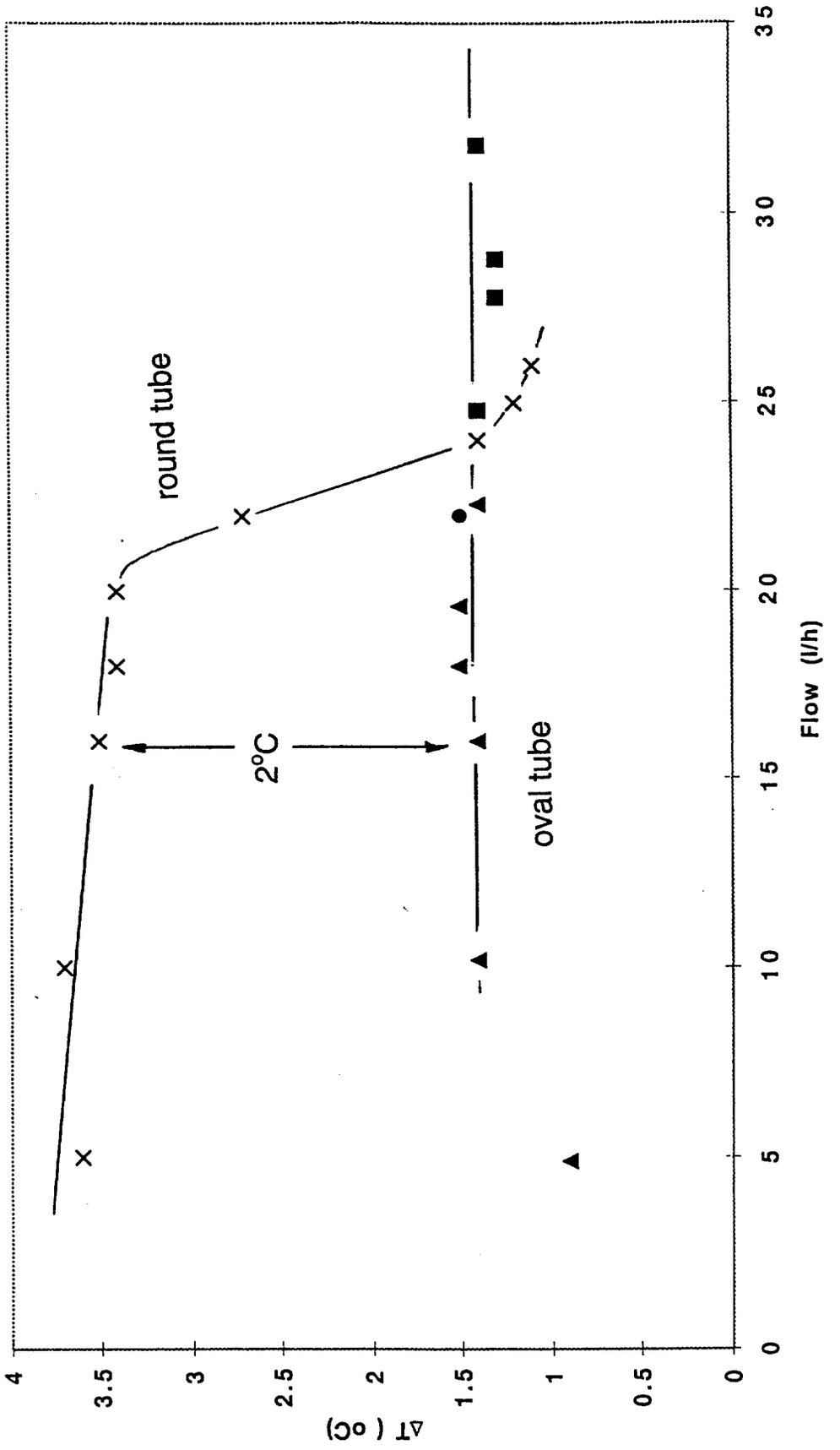


fig.8 Measurements of the cooling efficiency for a 1 meter long round tube with a 40W heat load as a function of the flux. At high flux the temperature difference becomes suddenly much smaller. It is believed that the regime is then turbulent. These data were collected at room temperature. With a 1.6 meter oval tube, at -10°C and 60W, the gradient is much smaller.

### 3.1.2 Oval tube

In order to reduce the temperature gradient in the coolant, the next tube iteration was oval or flat. as shown in fig.9. In addition to the smaller temperature gradient, this offers a large and simple thermal contact area to the module. This thermal contact is allowed to slide with a silicone compound, Dow Corning DC340, 50 μm thick. However this special silicone compound has still a poor thermal conductivity, between 0.42 W/mK, claimed by the manufacturer, 0.5 W/mK as measured at CERN (PPE94), 1.25 W/mK, as measured by the Mechanical & Electronic Engineering Division at Los Alamos (MEED92) and 0.82 W/mK as measured by us. Therefore a large contact area of about 5 $cm^2$ is considered in our design. For a module heat load of 5W, the expected thermal gradient across this silicone compound joint is expected to be rather small, ~ 0.5 K. This means that, even for a bad contact where only 50% of the surface touches or if the silicone compound thickness is 100 μm, the temperature difference between a good and a bad contact will be only 0.5 K. This is required to ensure the good reproducibility of the contact shown in our results.

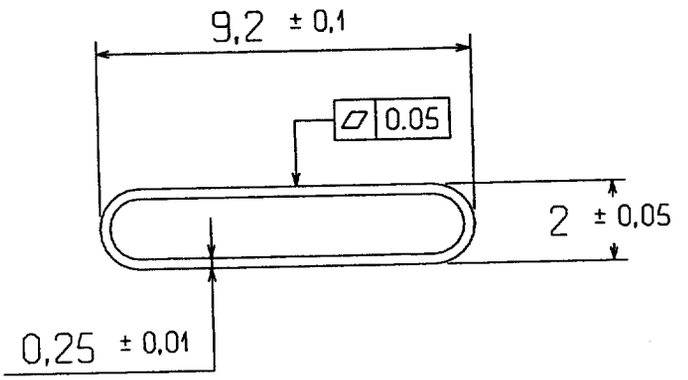


fig.9 The oval tube design.

The first oval tube was designed to allow for vacuum leak tests with a contraction of the flat surfaces of only 25 μm. The inner dimensions were 1.5x 8.75 mm2 and the wall thickness is 0.25 mm.

The use of this tube resulted in the expected improvement in cooling efficiency shown in fig. 8.
The apparatus used for this measurement is shown in fig. 10. Measurements of the cooling efficiency were performed with a heater wrapped around a 1.6m tube, which was cast into a u-shape aluminum profile, this heater bloc was then in contact with the oval tube with a silicone compound joint.

Because of the lack of viscosity data in the temperature region around -10 °C, the section of the tube was underestimated for low temperatures. Therefore, we measured a pressure drop of about ΔP≈300 mbar @ 13 l/h with a 33% glycol mixture. This is clearly outside specifications.

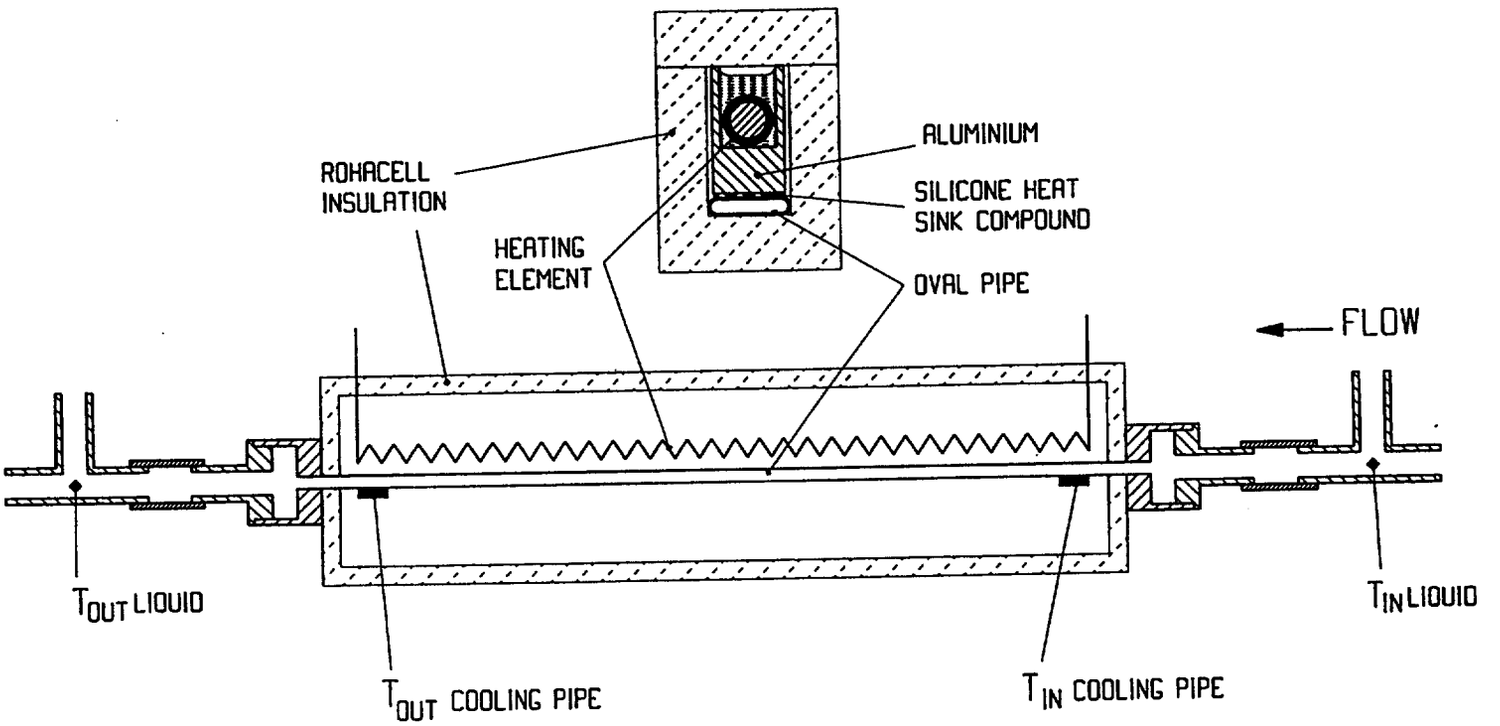


fig. 10. Apparatus used to measure the oval tube cooling efficiency. The tube was 1.6 meter in length and the heat load 60W.

However with the same tube and a mixture of methanol 24% by wt. (29%), we obtain:

table 1 Flow versus pressure at -10 and -16 °C

| Temp (°C) | ΔP (mbar) | Flow (l/h) |
|---|---|---|
| -10 | 300 | 22 |
| -16 | 330 | 18 |

The freezing point of this mixture is at -19°C, allowing to operation at temperatures much below -10°C. Even if this is not exactly within the specs, it is very close and we may have to consider a tube of 2 mm x 8.75mm inner dimension.

Measurements of the temperature gradient along the 1.6m tube with $\Delta P \approx 280$-295 mbar are shown in table 2 for the glycol mixture and table 3 for the methanol mixture.

table 2 Cooling results for glycol/water.

| W (watt) | $T_{in}$(°C) | $T_{out}$(°C) | $T_{air}$(°C) | flow (l/h) | $\Delta T$(°C) | $\Delta T_{th}$(°C) |
|---|---|---|---|---|---|---|
| 60 | -9.4 | -5.3 | -10.7 | 13.6 | 4.1 | 4.2 |

Note that the flow here are measured at room temperature after warming up the coolant at the exit of the tube, in order to avoid an unexpected temperature dependence of our "Pelton style" flowmeter used for measurements.

table 3 Cooling results for methanol/water.

| W (watt) | $T_{in}$(°C) | $T_{out}$(°C) | $T_{air}$(°C) | flow (l/h) | $\Delta P$ (mbar) | $\Delta T$(°C) | $\Delta T_{th}$(°C) |
|---|---|---|---|---|---|---|---|
| 60 | -9.8 | -7.4 | -10.1 | 22.3 | 293 | 2.4 | 2.5 |
| 60 | -16.1 | -13.1 | -11.5 | 18.4 | 326 | 3.0 | 3.1 |

With a measurement uncertainty of the temperature estimated to be about 0.2°C, the theoretical estimate, $\Delta T_{th}$°C, based on a trivial calculation, where all the heat of the heater goes into the glycol or methanol mixtures, is in excellent agreement with the data.

Note that the water/methanol mixture can be a safety issue and this will be debated soon.

The pressure drop was measured for the water/methanol mixture at various flows and temperatures as shown in fig. 11.

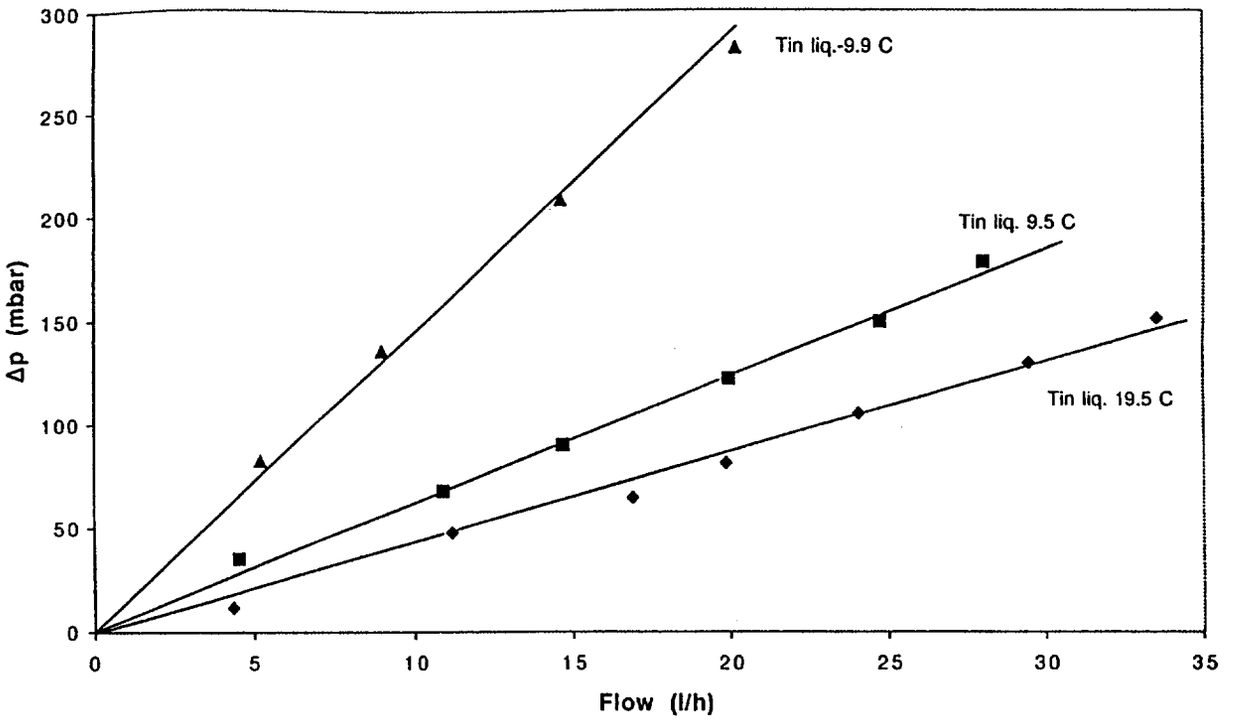


fig. 11. Pressure drop along the 1620 mm oval tube, c.f. fig. 9, described in this section, as a function of the flow at various temperatures $T_{in\ liq}$.

### 3.2 Thermal modules

Various thermal modules were built for thermal tests and metrology measurements. These modules all have heater blankets, 11.5x5.7cm$^2$ to simulate the heat generated by the detectors, up to 1W per module, as well as chip resistors to simulate the heat from the electronics on the boards, up to 4 W per module. For most thermal measurements, heat load of 1W per module onto the detectors and 4W per module onto the board were applied . These modules are described below in more details.

#### 3.2.1 Aluminum modules mock-up

Thirteen simple modules where build with aluminum plates for the detectors and board. The thickness of the plates was designed to match the thermal conductivity of the silicon detectors and of the BeO Z-module fan-in. These modules have one platinum resistor for temperature measurement near to the silicone compound joint with the cooling pipe, as shown in fig.12. The modules were essentially build to test the reproducibility of the cooling joints.

#### 3.2.2 $Al_2O_3$ Module

One module was built with fan-ins and boards made from $Al_2O_3$ and with heat radiator in AlN as shown in fig.13, The module was built to test the assembly method and to perform first thermal tests. The module was equipped with platinum resistors and heaters for thermal measurements.

#### 3.2.3 AlN Module

One module was built with fan-ins, boards and radiators made from AlN. This material offers an interesting advantage in comparison with other material, it has a CTE, $3 \bullet 10^{-6}/^{\circ}C$, which is close to that of silicon. Therefore little deformation is expected when the module is cooled, or when the modules have to be baked, minimizing thermal stresses. Note that the thermal conductivity of AlN, 170 W/mK @ 0°C, is not as high as that of BeO, 370 W/mK @ 0°C, but the machining of AlN is not toxic. The module was equipped with platinum resistors and heaters for thermal measurements as shown in fig.14.

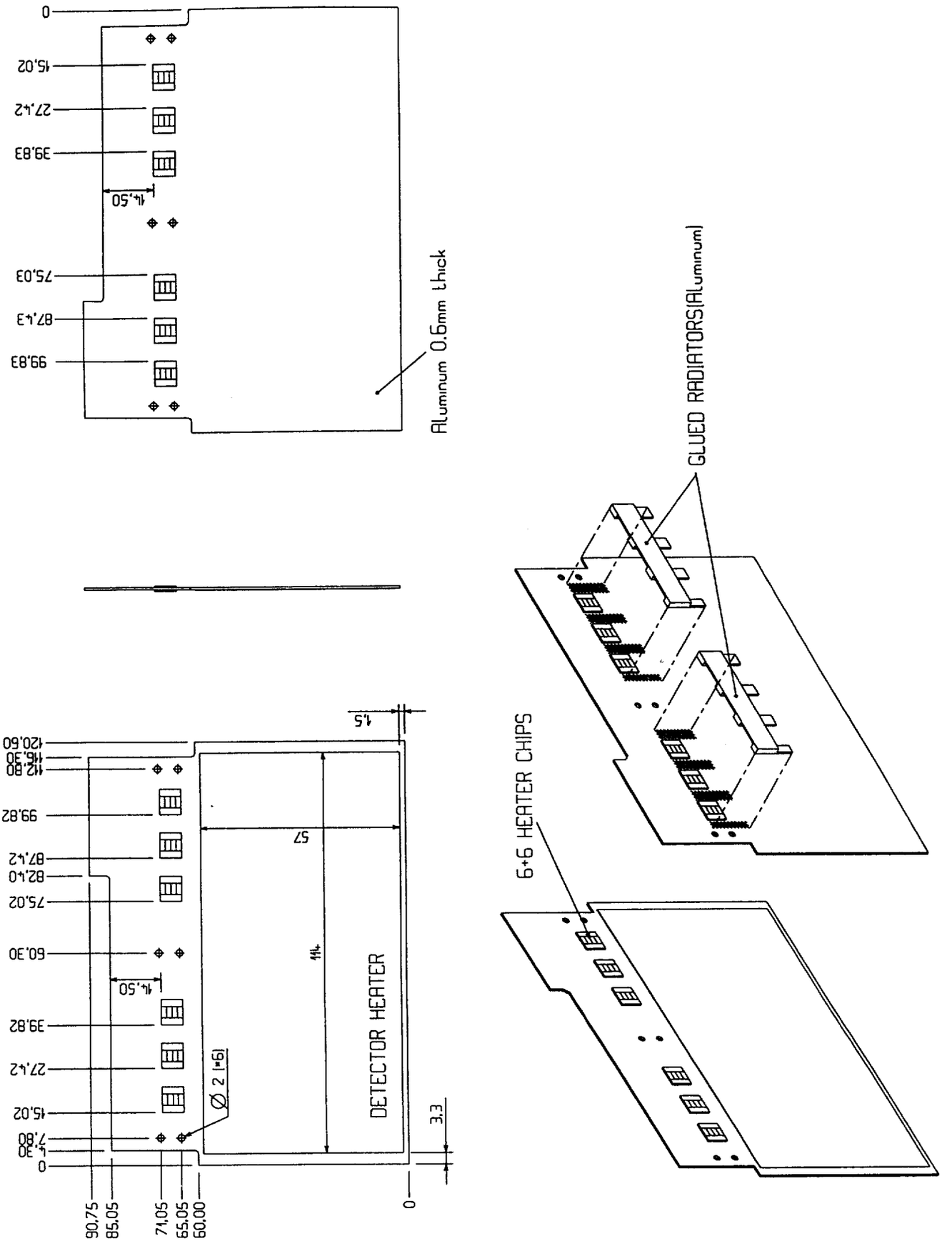


fig.12 Simple aluminum modules (Antico).

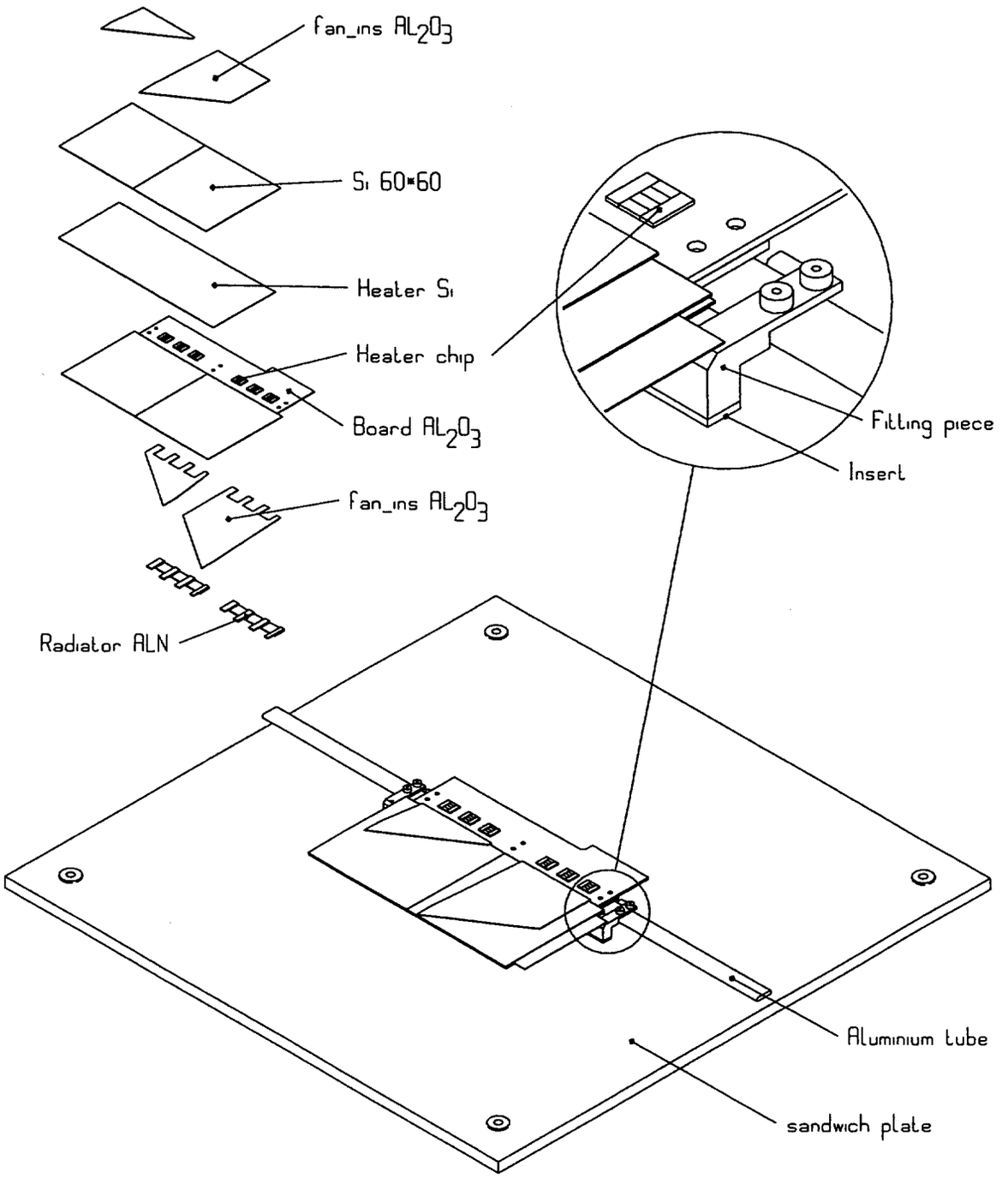


fig.13 $Al_2O_3$ module on a « two-module support ».

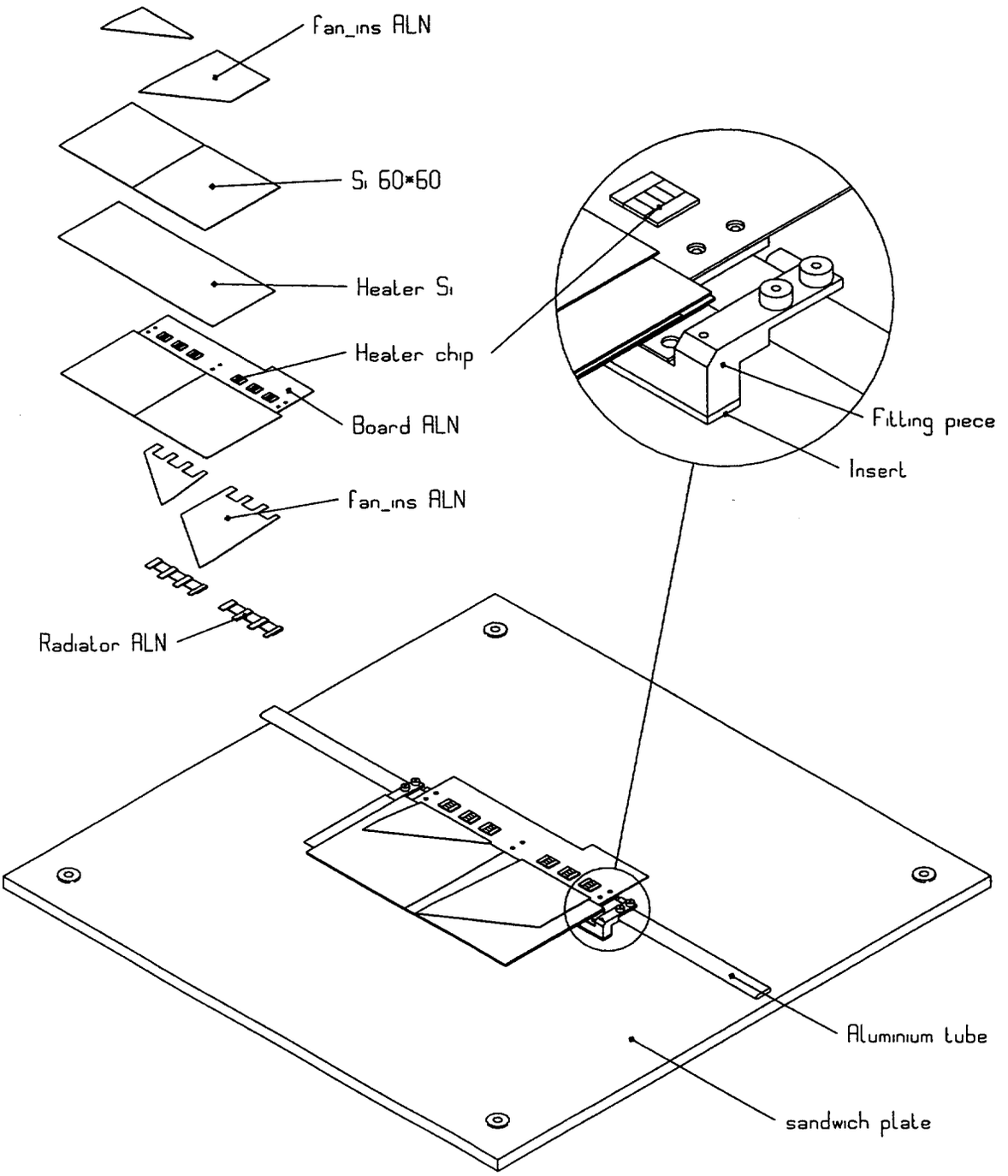


fig.14 AIN module on a « two-module support »..

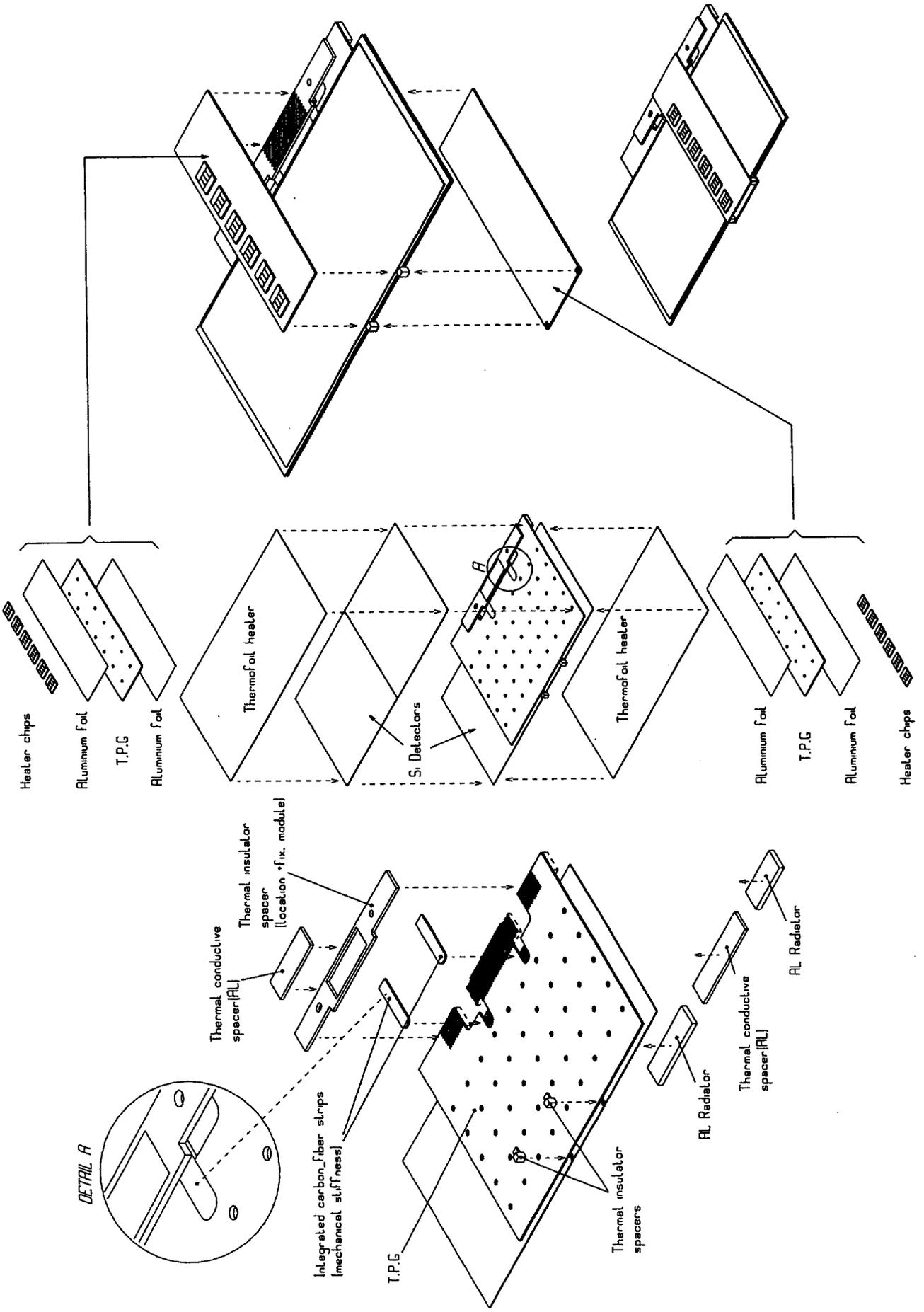


fig.15 TPG module.

### 3.2.4 TPG center-tap module

One module equipped with a high thermal conductivity core, TPG TC1050 from Advanced Ceramics Corporation (TPG97) was built, The thermal conductivity of TC1050 is about $\lambda \approx 1000$ W/mK and the radiation length is high, $X_0 = 43$ g/cm$^2$, $X_0 \bullet \rho = 19$ cm. We have chosen uncoated material and drilled holes in it, 1.7mm in diameter. This gives rigidity when the material is sandwiched between silicon detectors and glued with epoxy. The epoxy is then making pillars into the sandwich. The detector cooling was provided by a TPG plate, of thickness 500 μm and size, 70x100mm$^2$. Four dummy silicon plates, 300 μm x 60x60 mm$^2$, were glued on either sides of the TPG plate as shown in fig. 15. Contributions from the silicon detector to the total radiation length is 0.64% $X_0$. The additional contribution of this TPG plate is 0.26% $X_0$, i.e. 41% of the silicon contribution. The TPG plate could probably be made somewhat smaller to reduce the material budget. The board was also made from TPG, thickness: 500μm, size, 24x74mm$^2$, sandwiched between two Aluminum foil 50 μm thick. Since we were already using TPG, this was the simplest way to fabricate a high thermal conductivity board. High thermal conductivity ceramics could also serve as the board. The rest of the module was made from aluminum for initial thermal tests.

An interesting feature of this module assembly is a "bridge" which can be aligned precisely with respect to the detectors during the assembly procedure, allowing an accurate positioning of the module to the supports. This implies that no accurate alignment steps is required on the hybrid.

### 3.3 Two-modules setup.

A small carbon sandwich plate, with carbon fiber/cyanate ester honeycomb and skins, was built with inserts to perform the first thermal measurements using one or two modules. The setup is shown in figs.12 and 13. One of the problem encountered with this apparatus was the poor stability of the tube, which produces poor thermal contact. This problem was solved by adding a guiding structures on both sides of the plate.

### 3.4 Full length prototype

A large carbon fiber sandwich plate, with Nomex® honeycomb core, was built with inserts machined to a precision of <10μm. Supports were mounted onto the inserts, as shown in fig. 16 This structure was used to perform thermal measurements with the modules described above and metrology measurements when the whole assembly was thermally cycled, or cooled.

### 3.5 Experimental arrangement.

The thermal measurements were performed in a large freezer, 1.78m in length, at a standard air temperature around -10°C. A cooling unit was providing coolant at temperatures between -20°C and room temperature. A schematic representation of the apparatus is shown in fig.17. The pressure drop along the cooling pipe was measured as well as the flow. Note that the flow measurement was made at room temperature when the coolant was warmed up to room temperature with a heat gun. This was necessary with the Pelton style flow-meter we used, since it shows a temperature, or viscosity dependence.

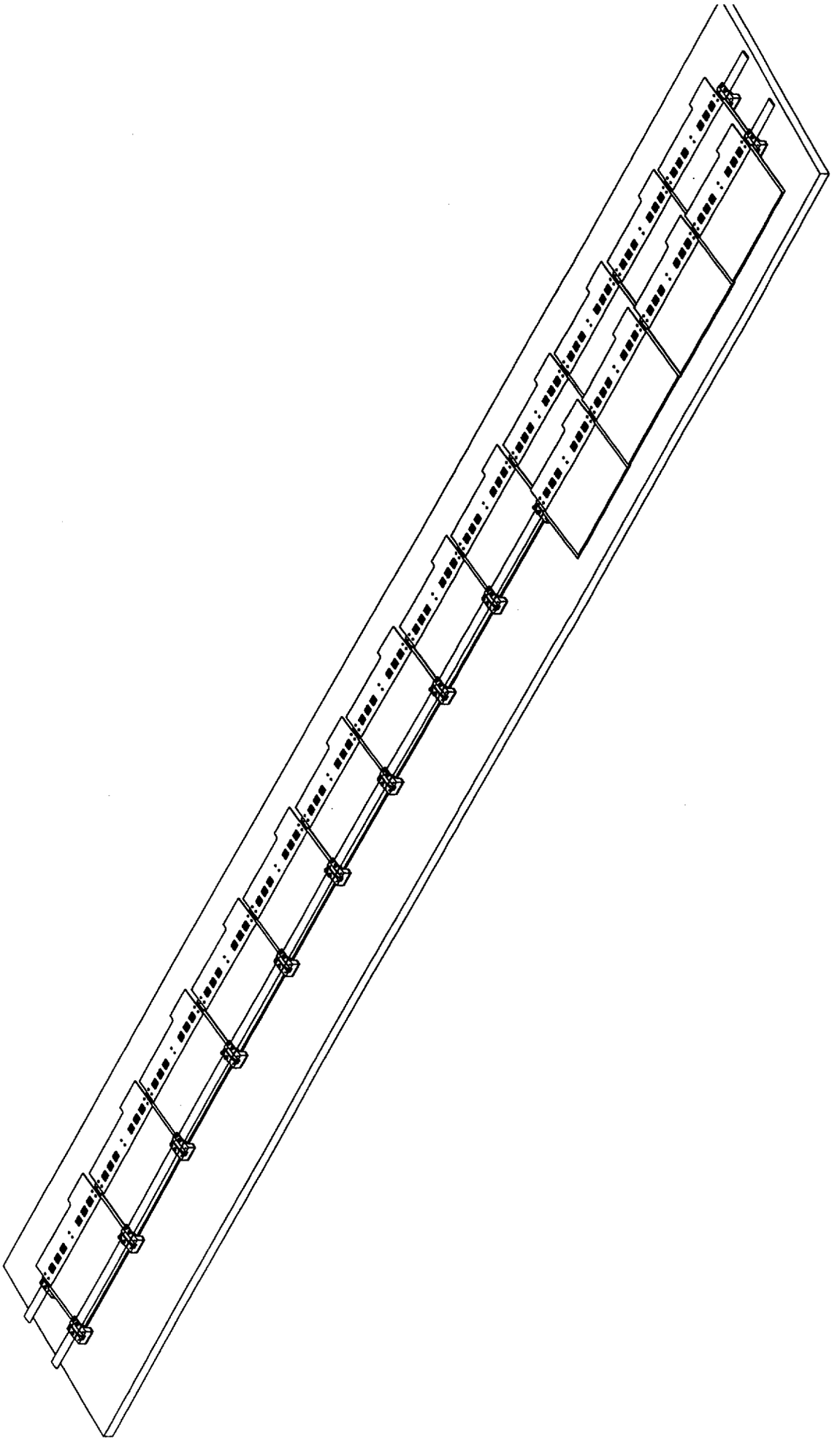

fig.16 Full length prototype.

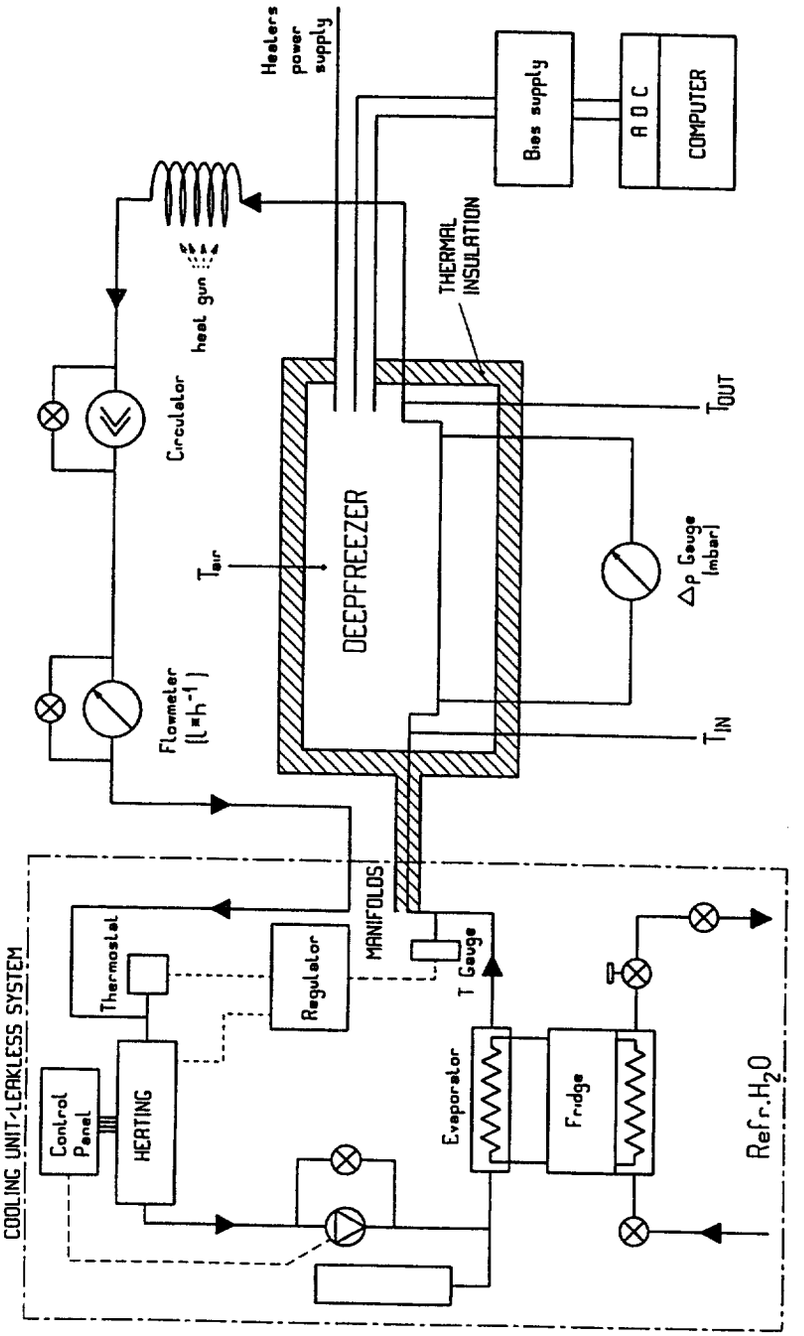


fig.17 Experimental arrangement, including the cooling unit, pressure gauge, flow-meter, freezer and the heat gun used to warm the coolant before the flowmeter.

Temperature measurements were performed with a platinum resistor, PT100 (100Ω at 0°C. A stabilized DC 10 V bias supply was used with another high stability resistor of 2kΩ to reduce the voltage to about 0.5 V on the PT100 terminals as shown in fig. 18. The temperature dependent voltage on these terminals was measured with a 16-channel ADC card in a Macintosh. A labview® program was used for the data acquisition. Calibration of the electronics and cables was performed in a mixture of water and ice at 0°C for all the channels. Since small differences between the PT100 were observed, up to 0.3°C, small corrections were applied to compensate when necessary. The measurement errors for all the temperature measurements was estimated to be ±0.2 °C. The heat dissipated by the PT100, about 2.5 mW, did not affect the measurements. Therefore the simple circuit shown in fig. 18 was used. For a higher accuracy a bridge with differential ADC readout would be recommended as well as other calibration procedures. This method was not adopted to save ADC channels.

A bias supply provided DC current to the module heaters. Both the currents and the voltages were measured to determine the heat load on the modules.

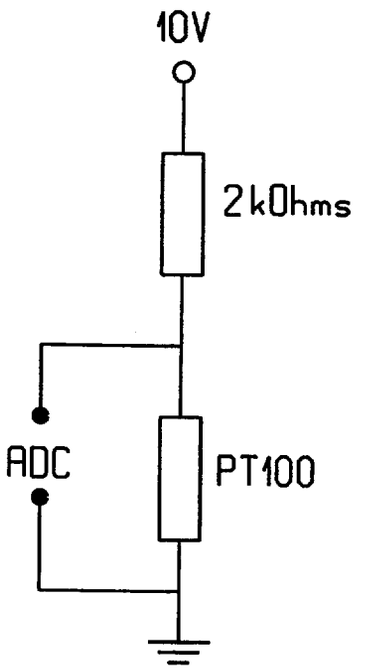


fig. 18 Electrical diagram used to measure the temperature.

## 3.6 Results

### 3.6.1 Full length prototype

The reproducibility of the silicone compound joint was tested three times on 13 dummy aluminum modules. The silicone compound was completely removed and the new silicone compound layers, 50 μm thick, were replaced two times. In one case modules were permuted and one run was at -14°C. Most data points were measured twice. The silicone

compound joints appear to be very reproducible. The data of figs. 19 and 20 show that within 0.4 degree, the silicone compound joint is reproducible. There is one exception on the sides of the row where the cooling pipe was not well fixed. This problem was already mentioned earlier, and shows again that it is mandatory to guide the tube on both side. Due to differences in the construction of the modules, heater locations and positions of the platinum resistors, the temperatures measured on the modules are different for different modules. These differences are of the order of 1 degree and are larger than that observed for a module after it has been removed. To demonstrate this, the modules were not always installed at the same location. In order to compare the results, we plotted in fig.19, the temperature differences between the modules and the expected coolant temperature at the module positions.

Observation of the silicone compound after removal has shown that the modules were sometimes not in contact over the whole area because of a misalignment of the flat tube plane with respect to the radiator plane. An area of up to about 50% not in contact, did not significantly affect the results.

### 3.6.2 Module cooling

The cooling measurements were performed with a heat load of 1 W for the detector heater blankets and 4W for the « chips on the board ». For the 3 types of modules, platinum resistors were used to measure the temperature in different positions on the modules, as shown in figs.19 to 22. For the TPG module, an additional measurement was performed with an insulator in the 500μm gap between the electronic board and the detector. For this measurement we have chosen a GoreTex® blanket, 450μm thick. The temperatures of the $Al_2O_3$ module are clearly higher than these from the other module because the thermal conductivity of the ceramic is not a high as that of AlN. TPG shows an even lower temperature than AlN for the same reason but also because of a different construction as shown in fig.15. The maximum detector temperature is listed in table 3. Clearly the TPG module with GoreTex® offers the best results. At this point we do not know if this material is well suited for its radiation hardness or for its radiation length. It was considered interesting here for its mechanical properties but another material could be used.

table 3 : Temperature difference between the mean fluid temperature of the coolant and the hottest detector temperature.

| | $Al_2O_3$ | AlN | TPG | TPG GoreTex® |
|---|---|---|---|---|
| $\Delta T$ [K] | 7.1 | 6.2 | 5.9 | 5.4 |

Using the best TPG figure, it seems that a temperature difference of 5.4 degrees can be obtained between the hottest detector point on the module and the fluid temperature.

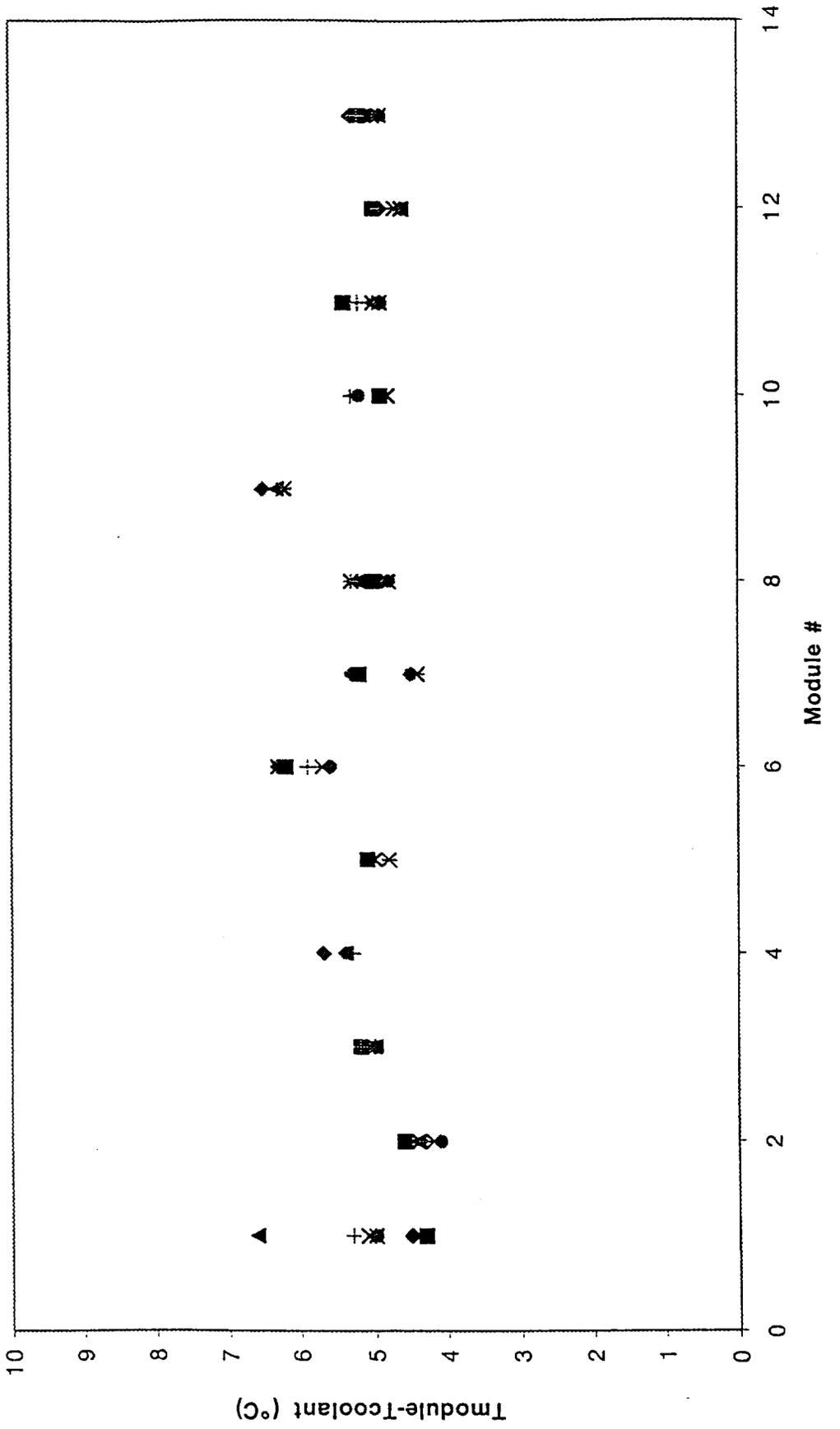


fig.19 Reproducibility data of the silicone compound joints.

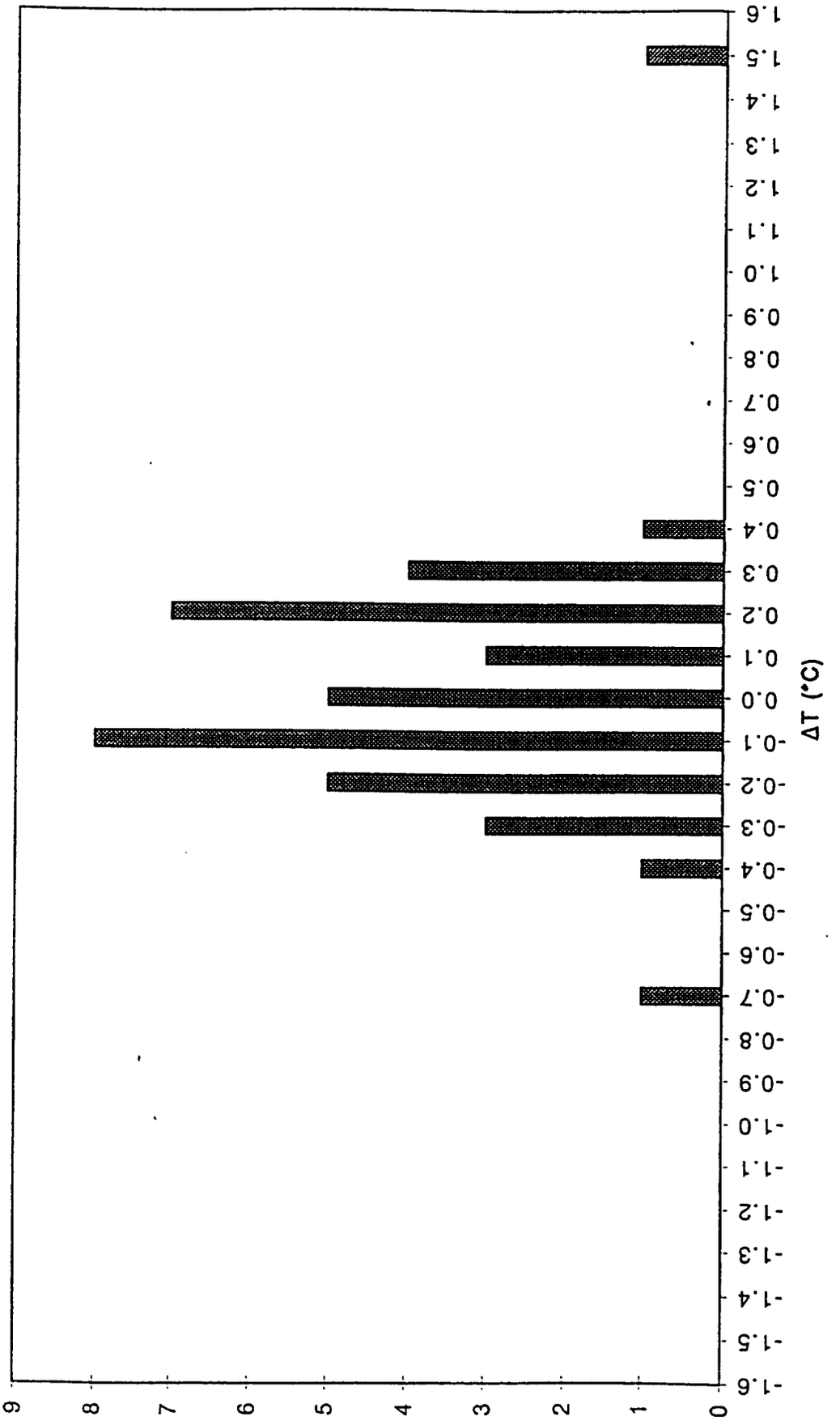


fig. 20. Reproducibility distribution of the temperature. The reproducibility data of the previous figure are averaged for each module. The temperature difference about the mean after reinstallation and removal of the heat sink compound is shown. Except for the two values at -0.7 and 1.5 °C which are caused by a poor tube guiding, all the joints were reproduced within +/- 0.4 °C with a standard deviation of about 0.2 °C.

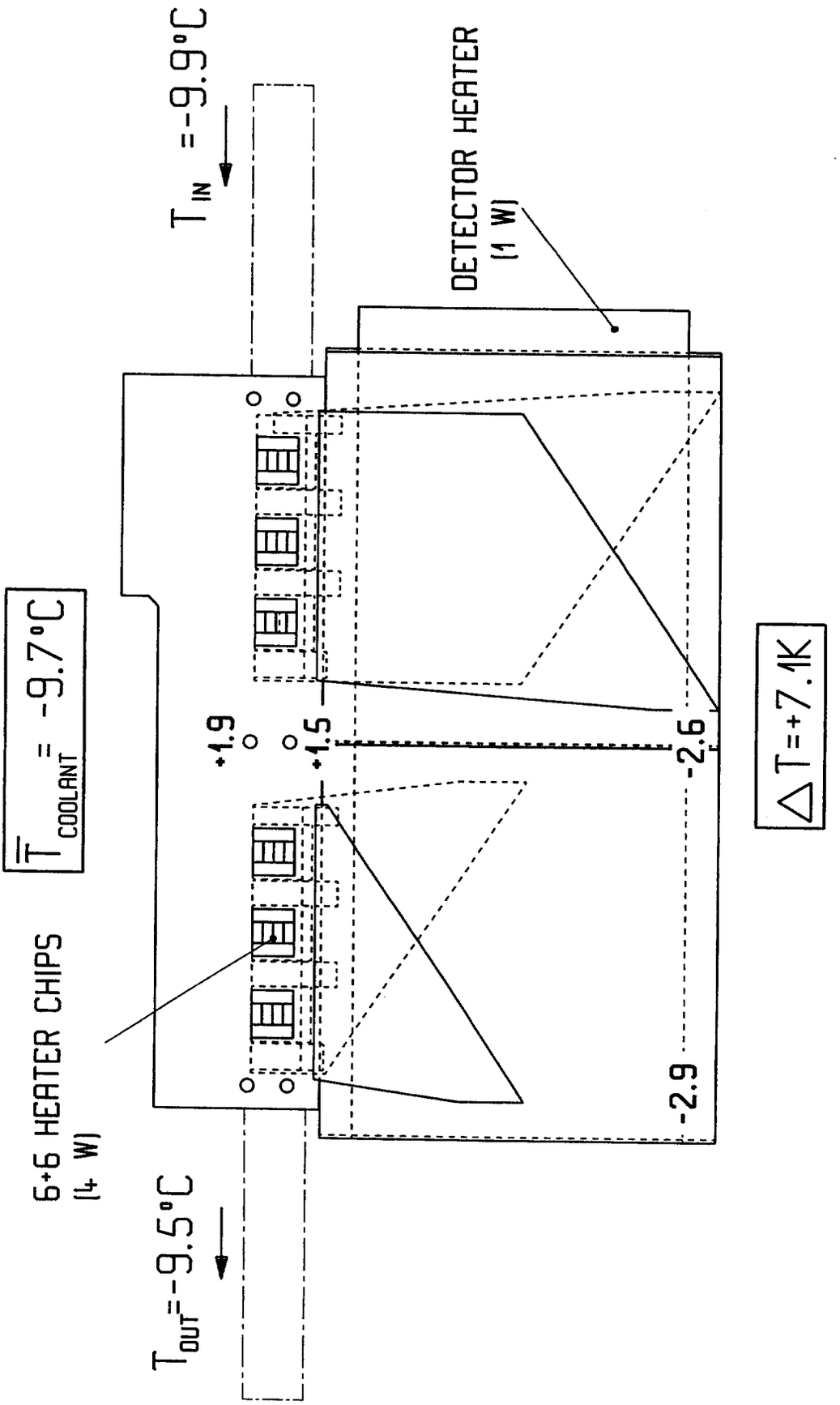


fig. 21 Temperature profile of the $Al_2O_3$ module.

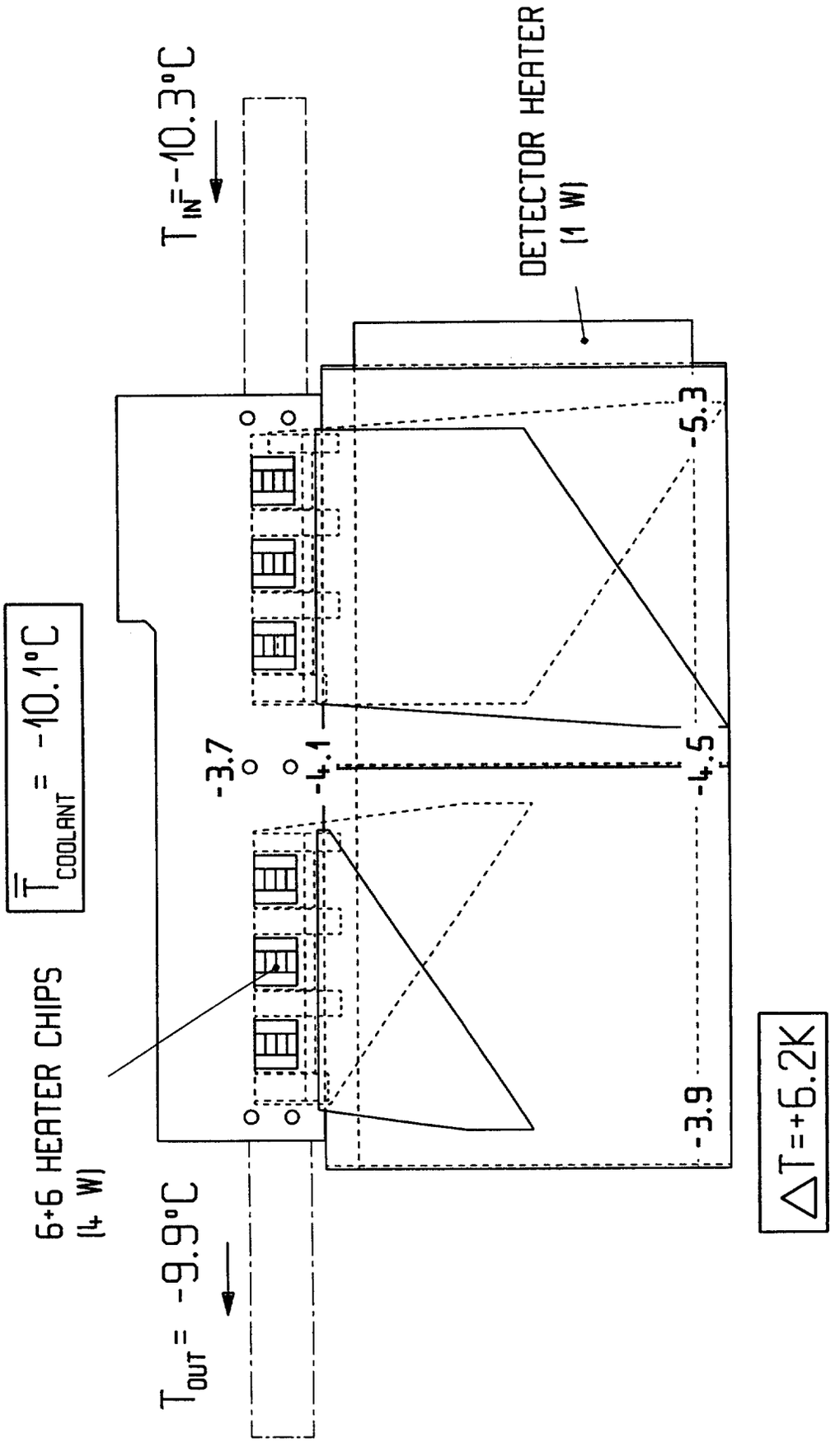


fig. 22 Temperature profile of the AIN module.

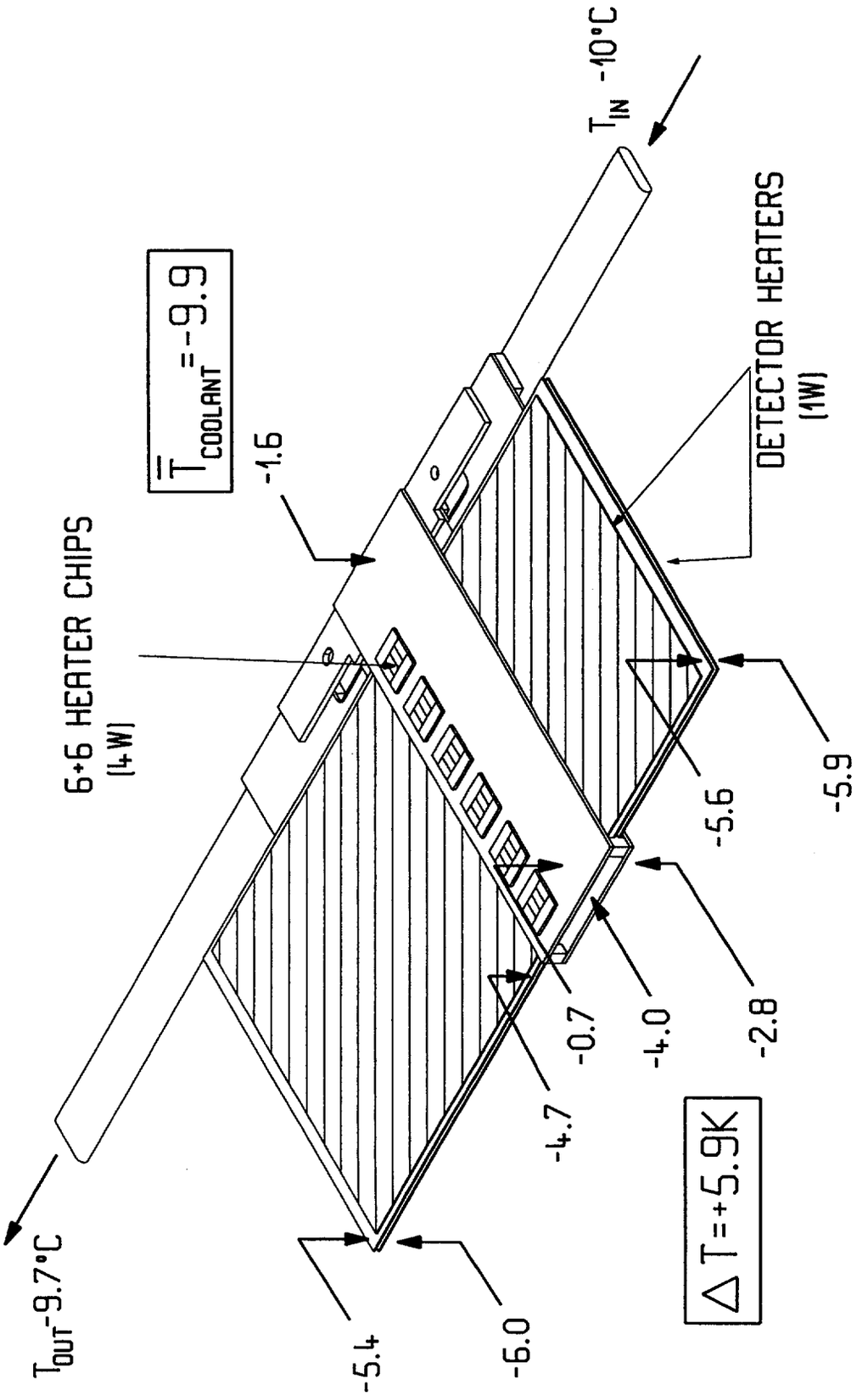


fig. 23 Temperature profile of the TPG module.

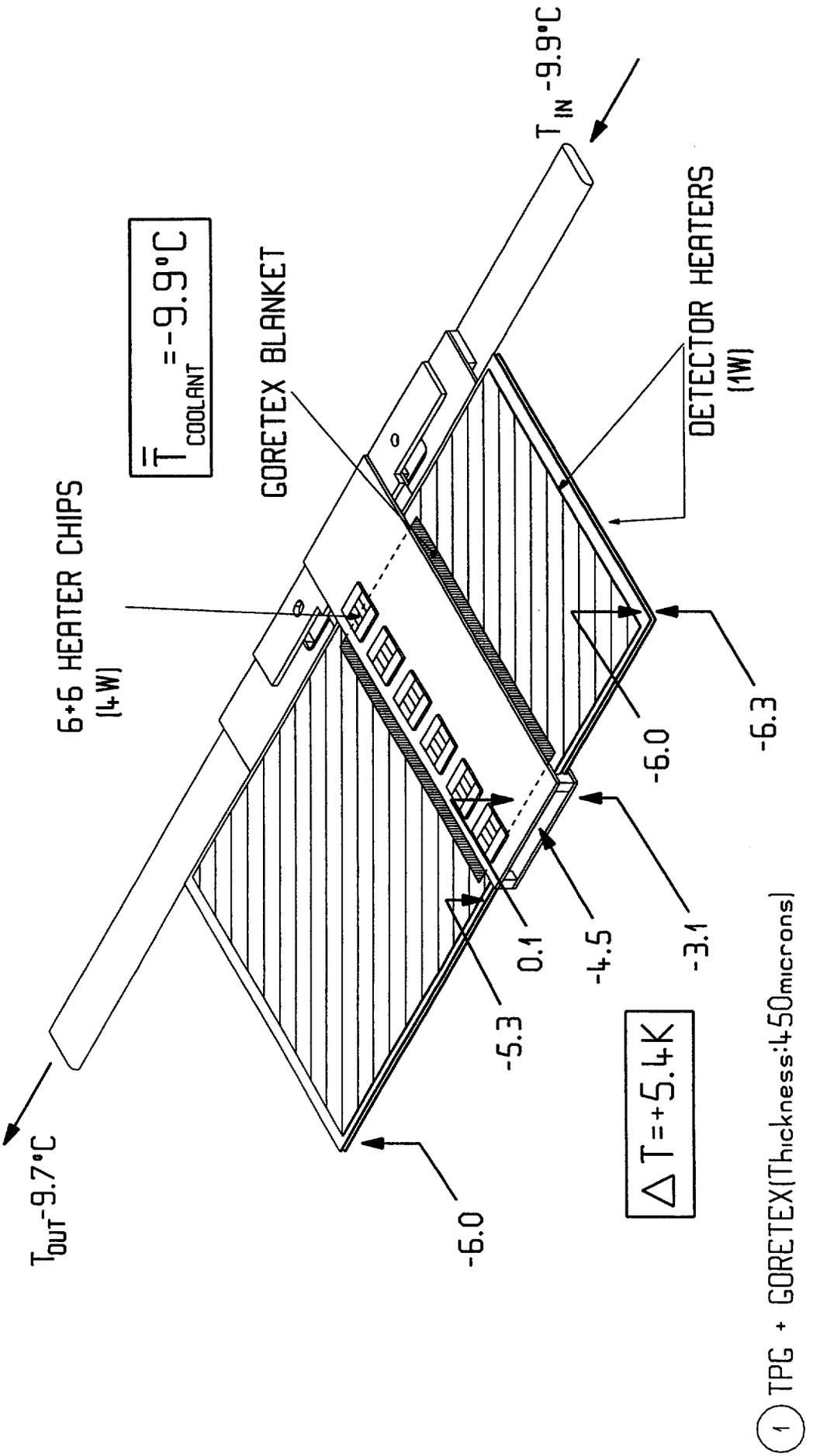


fig. 24 Temperature profile of the TPG module with a Gore-Tex® blanket.

## 5 Radiation hardness

A radiation hardness test of the silicon heat sink compound Dow Corning 340 has been completed. With a total fluence of $6 \bullet 10^{13}$ neutrons/cm$^2$ no significant change in the thermal conductivity was seen and the texture of the grease was unchanged (PPE94)

Further tests of the heat sink compound joint are under progress, where a pile of 11 joint, aluminum/compound, will be irradiated. First results indicate that the thermal conductivity is 0.82 W/mK before irradiation.

The radiation induced corrosion of the aluminum pipe filled with a coolant is planned for this year.

## 4 Conclusion

The zero CTE mechanical structure presented here will permit precise mounting of modules over a large temperature range. The cooling system can be adapted to any module styles: Z r-$\varphi$ or center-tap. We have demonstrated the clear improvement of oval cooling tubes as compared to round tubes as well as the good reproducibility of the sliding silicone compound joints between the cooling tube and the modules. The cooling system used here, with a mixture of methanol/water, is an interesting simple and robust alternative to the binary ice options but does have a greater $\Delta$T. However the choice about the cooling fluid is not crucial since both methods require similar specifications for the tube impedance.

Various types of thermal modules have been investigated. For the center-tap module a TPG core has been used to keep the detector cool. This center-tap module has shown good thermal properties. Even with a simple cooling system as the one used here, it is possible to keep the detector temperature below -5°C with a coolant temperature at the entrance of the barrel at -14°C and with a temperature gradient along the tube of a few degrees.

A manifold prototype is under construction, in order to demonstrate that such a leakless cooling system can operate reliably without individual tube flow controls.

A complete metrology survey of the full length prototype will be performed to show that such a structure has the required stability when thermally cycled between room temperature and -15°C.

## Acknowledgment :

We are very grateful to Advanced Ceramics corporation for providing customized TPG plates.

## References:

ATL94 Atlas Technical Proposal, CERN/LHCC/94-43, LHCC/P2 (1994).

TPG97 Advances Ceramics corporation, P.O.B. 94924, Cleveland, Ohio USA 44101-4924.

LCS Leakless Cooling System, M Bosteels.

Bon94 P. Bonneau, Note technique, MT-SM/94-13 (1994).

Bon95 P. Bonneau et al, MT-SM/95-(1995).

MEED92 Mechanical & Electronic Engineering Division at Los Alamos, MEE 12-92-289

PPE94 A. Onnela et al., Technical note CMS-TN/94-248, TA1/94-24.